Scanning for New BRI1 Mutations via TILLING Analysis[1]

Chao Sun,[a] Kan Yan,[a,2] Jian-Ting Han,[a] Liang Tao,[a] Ming-Hui Lv,[a] Tao Shi,[a] Yong-Xing He,[a] Michael Wierzba,[b] Frans E. Tax,[b] and Jia Li[a,3]

[a]Ministry of Education Key Laboratory of Cell Activities and Stress Adaptations, School of Life Sciences, Lanzhou University, Lanzhou 730000, China
[b]Department of Molecular and Cellular Biology, University of Arizona, Tucson, Arizona 85721

ORCID IDs: 0000-0002-1386-3310 (F.E.T.); 0000-0002-3148-6897 (J.L.).

The identification and characterization of a mutational spectrum for a specific protein can help to elucidate its detailed cellular functions. BRASSINOSTEROID INSENSITIVE1 (BRI1), a multidomain transmembrane receptor-like kinase, is a major receptor of brassinosteroids in Arabidopsis (*Arabidopsis thaliana*). Within the last two decades, over 20 different *bri1* mutant alleles have been identified, which helped to determine the significance of each domain within BRI1. To further understand the molecular mechanisms of BRI1, we tried to identify additional alleles via targeted induced local lesions in genomes. Here, we report our identification of 83 new point mutations in *BRI1*, including nine mutations that exhibit an allelic series of typical *bri1* phenotypes, from subtle to severe morphological alterations. We carried out biochemical analyses to investigate possible mechanisms of these mutations in affecting brassinosteroid signaling. A number of interesting mutations have been isolated via this study. For example, *bri1-702*, the only weak allele identified so far with a mutation in the activation loop, showed reduced autophosphorylation activity. *bri1-705*, a subtle allele with a mutation in the extracellular portion, disrupts the interaction of BRI1 with its ligand brassinolide and coreceptor BRI1-ASSOCIATED RECEPTOR KINASE1. *bri1-706*, with a mutation in the extracellular portion, is a subtle defective mutant. Surprisingly, root inhibition analysis indicated that it is largely insensitive to exogenous brassinolide treatment. In this study, we found that *bri1-301* possesses kinase activity in vivo, clarifying a previous report arguing that kinase activity may not be necessary for the function of BRI1. These data provide additional insights into our understanding of the early events in the brassinosteroid signaling pathway.

Brassinosteroids (BRs) are known to play critical roles in regulating many aspects of plant growth and development, including germination, cell elongation, flowering time control, reproduction, photomorphogenesis, and skotomorphogenesis (Clouse and Sasse, 1998; Gudesblat and Russinova, 2011; Wang et al., 2012; Zhu et al., 2013). Recent studies revealed that BRs also are involved in many additional physiological processes, such as root meristem maintenance (González-García et al., 2011; Hacham et al., 2011; Vilarrasa-Blasi et al., 2014; Chaiwanon and Wang, 2015; Wei and Li, 2016), stomatal development (Gudesblat et al., 2012; Kim et al., 2012), root hair differentiation (Cheng et al., 2014), leaf angle regulation in monocots (Zhang et al., 2012), shoot branching control (Wang et al., 2013), and organ boundary determination (Bell et al., 2012; Gendron et al., 2012).

In Arabidopsis (*Arabidopsis thaliana*), BRs are perceived by their major receptor BRASSINOSTEROID INSENSITIVE1 (BRI1) and coreceptor BRI1-ASSOCIATED RECEPTOR KINASE1 (BAK1), both of which are single-pass transmembrane Leu-rich repeat receptor-like protein kinases (LRR-RLKs; Li and Chory, 1997; Li et al., 2002; Nam and Li, 2002; Gou et al., 2012). There are 25 total extracellular LRRs in BRI1. Between the 21st and 22nd LRRs, there is an amino acid sequence containing 68 residues that is termed an island. Genetic and structural analyses indicated that the island and the 22nd LRR are involved directly in BR binding. In the absence of BRs, the kinase activity of BRI1 is inhibited by its C terminus (Wang et al., 2005) and by its associated inhibitory protein, named BRI1 KINASE INHIBITOR1 (BKI1; Wang and Chory, 2006). When BRs are present, on the other hand, they can interact directly with the extracellular pocket of BRI1, causing BKI1 to dissociate from the complex (Wang and Chory, 2006; Hothorn et al., 2011; She et al., 2011; Wang et al., 2014). The newly formed BRI1-brassinolide (BL) surface can interact directly with the extracellular residues of BAK1 via several hydrogen bonds (Santiago et al., 2013; Sun et al., 2013). The BRI1-BL-BAK1 complex can then initiate early BR signaling events and activate its downstream signaling cascade

[1] This work was supported by the National Natural Science Foundation of China (grant nos. 31530005 and 31470380 to J.L.).

[2] Current address: School of Chemical and Biological Engineering, Lanzhou Jiaotong University, Lanzhou 730000, China.

[3] Address correspondence to lijia@lzu.edu.cn.

The author responsible for distribution of materials integral to the findings presented in this article in accordance with the policy described in the Instructions for Authors (www.plantphysiol.org) is: Jia Li (lijia@lzu.edu.cn).

J.L. and F.E.T. conceived the research plans, supervised the experiments; C.S. designed the experiments, analyzed the data; C.S. and K.Y. performed most of the experiments; L.T., M.-H.L., and M.W. performed part of the experiments; J.-T.H. and Y.-X.H. performed the molecular dynamic simulation analysis; T.S. helped with the sequence analysis; C.S. and J.L. wrote the article.

www.plantphysiol.org/cgi/doi/10.1104/pp.17.00118

(Wang et al., 2008). Genetic and structural analyses demonstrated the essential roles of both BRI1 and BAK1 in controlling BR signal transduction (Clouse et al., 1996; Li and Chory, 1997; Hothorn et al., 2011; She et al., 2011; Gou et al., 2012; Santiago et al., 2013; Sun et al., 2013).

During the past two decades, over 20 unique *bri1* alleles have been isolated (Clouse et al., 1996; Li and Chory, 1997; Noguchi et al., 1999; Friedrichsen et al., 2000; Xu et al., 2008; Belkhadir et al., 2010; Shang et al., 2011; Gou et al., 2012). Analyses of these mutants have contributed significantly to our better understanding of BRI1 in regulating plant growth and development (Vert et al., 2005). These alleles share similar phenotypes in various degrees, including dwarfism, dark-green, compact rosette leaves with short petioles, delayed flowering time and senescence, reduced male fertility, and altered photomorphogenesis and skotomorphogenesis (Clouse, 1996; Kwon and Choe, 2005). Most alleles exhibiting the strongest morphological defects contain point mutations in the island or kinase domain (Friedrichsen et al., 2000). BRI1 was first cloned via a map-based strategy (Li and Chory, 1997). Many of the early isolated *bri1* alleles are strong alleles with largely reduced male sterility, preventing their use in large-scale genetic transformation assays. Fertile weak *bri1* alleles, such as *bri1-5* and *bri1-9*, on the other hand, are excellent genetic tools used for characterizing the entire BR signaling pathway via extragenic modifier screens (Noguchi et al., 1999). For example, several key components regulating BR signal transduction or BR homeostasis were identified via activation-tagging genetic screens using *bri1-5* as background, including BRS1 (Li et al., 2001a), BAK1 (Li et al., 2002), BSU1 (Mora-García et al., 2004), BRL1 (Zhou et al., 2004), BEN1 (Yuan et al., 2007), and TCP1 (Guo et al., 2010). EBS1 to EBS7, a series of functionally related proteins mediating endoplasmic reticulum (ER) quality control, were isolated via a suppressor screen from ethyl methanesulfonate (EMS)-mutagenized *bri1-9* (Jin et al., 2007, 2009; Su et al., 2011, 2012; Hong et al., 2012; Liu et al., 2015). BES1, a key downstream transcription factor in the BR signaling pathway, was identified via a suppressor screen utilizing an EMS-mutagenized *bri1-119* library (Yin et al., 2002). Identification of these key regulatory components using weak *bri1* mutants has contributed significantly to our current knowledge of the BR signaling pathway, from BR perception to downstream-responsive gene regulation.

In order to deeply understand the molecular mechanisms of BRI1 in regulating the BR signaling pathway, we analyzed all *BRI1* point mutations generated from a targeted induced local lesions in genomes (TILLING) project (McCallum et al., 2000). Among 83 total *BRI1* point mutations isolated, we identified nine mutants, including four subtle, one weak, and four strong alleles. For example, *bri1-702* is a new weak allele with a mutation in the activation loop of the BRI1 kinase domain. Several previously identified *bri1* activation loop point mutants are all strong alleles. Therefore, *bri1-702* represents the first weak allele bearing a point mutation in the activation loop. *bri1-705* is a new subtle allele containing a point mutation in the extracellular portion. Structural analysis suggests that this mutation likely disrupts the formation of hydrogen bonds among BRI1, BL, and BAK1. A third interesting mutant is *bri1-706*, containing a point mutation in the eighth LRR of the extracellular portion of BRI1. *bri1-706* shows a subtle aerial part defective phenotype compared with wild-type plants, but its root growth is largely insensitive to exogenously applied BL. The new mutants identified from these studies can be used as genetic tools to further dissect the functions of BRI1 as well as utilized as references to study the biological functions of other RLKs in plants.

RESULTS

A Series of New *bri1* Alleles Were Identified via TILLING Analyses

BRI1, the major receptor of BRs in Arabidopsis, contains multiple functional domains (Li and Chory, 1997; Friedrichsen et al., 2000). Mutational analyses have helped to characterize the biological significance of each of these domains. To further dissect the roles of BRI1 in the BR signaling pathway, we tried to identify all possible *BRI1* mutations and identify the mutants with altered phenotypes.

TILLING is a reverse genetic method using a high-throughput screening technology to detect point mutations from an EMS-mutagenized library (McCallum et al., 2000). Using this approach, a large number of mutations can be isolated for a specific target gene. TILLING has been used to generate mutations for a number of important genes, including *BRI1* in Arabidopsis (Till et al., 2003). All 87 *BRI1* TILLING mutations were obtained from the Arabidopsis Biological Resource Center, and 83 mutations were confirmed by a derived cleaved-amplified polymorphic sequence (dCAPS) method (Neff et al., 1998). These mutations are distributed throughout the entire BRI1 sequence, especially in LRR1 to LRR10 of its extracellular portion, island, and kinase domain (Supplemental Fig. S1). These mutations were generated in the Columbia-0 (Col-0) background containing an *er* mutation. A high dose of EMS could introduce mutations in other genes that could result in BRI1-unrelated phenotypes. In order to remove those additional mutations, we backcrossed the mutants with Col-0 for at least three generations. Offspring plants containing *BRI1* mutations were selected using the dCAPS approach (Neff et al., 1998). After backcrossing three times, most mutations were found to exhibit no morphological differences from wild-type plants. Only nine mutations consistently exhibit typical *bri1*-like phenotypes. These mutants were named in the order of their identification, from *bri1-702* to *bri1-711* (Fig. 1; Table I).

To further confirm their *bri1*-related phenotypes, we carried out two additional backcrosses for the nine new mutants isolated via TILLING. In the F2 generation of the third backcrossing, the phenotypes of *bri1-702*, *bri1-705*,

bri1-706, *bri1-710*, and *bri1-711* were segregated out as single recessive alleles with a ratio close to 3:1. However, for strong alleles, the ratio is less than 4:1, which might be caused by lower germination rates, as observed previously (Steber and McCourt, 2001). Thus, the phenotype appears to be caused by a single locus for all nine different mutants. *bri1-702* shows a weak *bri1* phenotype similar to *bri1-5*, *bri1-9*, and *bri1-301* (Fig. 2A; Noguchi et al., 1999; Xu et al., 2008). In comparison, *bri1-705*, *bri1-706*, *bri1-710*, and *bri1-711* show even weaker phenotypes than *bri1-702*, which, therefore, were named as subtle alleles in this study. On the other hand, *bri1-703*, *bri1-704*, *bri1-708*, and *bri1-709* show severe phenotypes similar to a previously reported *bri1* null allele, *bri1-701* (Fig. 2A; Gou et al., 2012). Interestingly, *bri1-707* and *bri1-301* both have mutations in Gly-989, but with different amino acid substitutions. As a consequence, *bri1-301* shows a weak *bri1* phenotype (Xu et al., 2008), whereas *bri1-707* does not show any defective phenotypes. Similarly, *bri1-708* and *bri1-8/108-112* bear different mutations at the same residue. While *bri1-8/108-112* are intermediate *bri1* mutants (Noguchi et al., 1999), *bri1-708* shows a null *bri1* phenotype (Fig. 2A). Statistically, all nine of these new *bri1* mutants show significantly reduced growth (Fig. 2B).

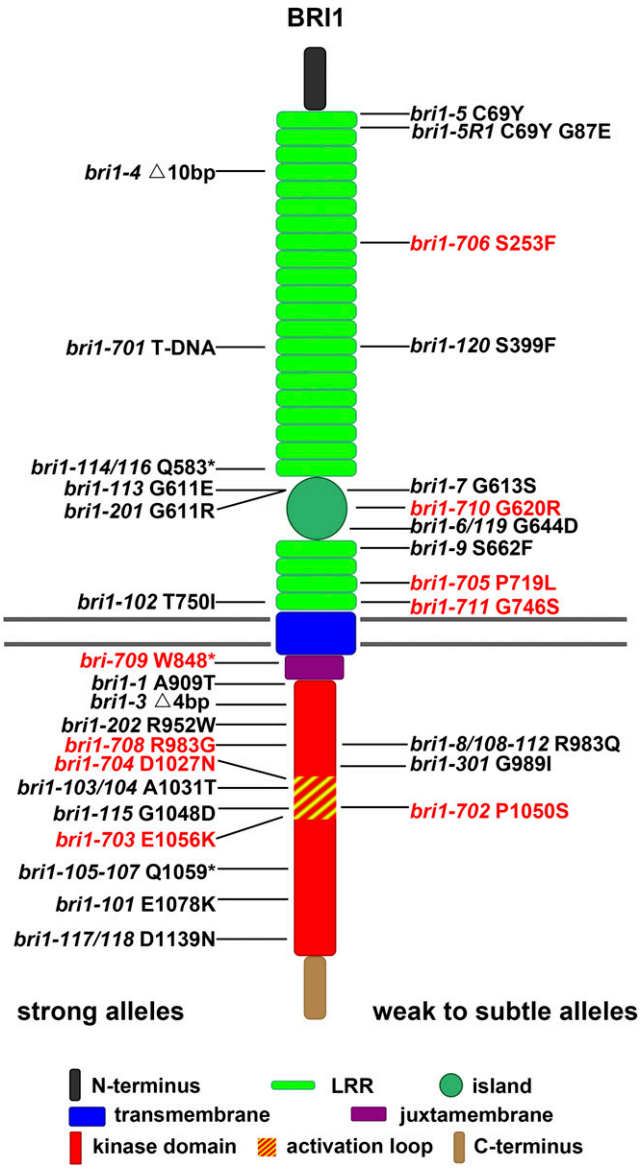

Figure 1. Diagram showing all *bri1* mutants identified thus far, including nine new alleles identified by this study. New mutants are labeled in red, and known mutants are labeled in black. Known *bri1* mutants include *bri1-1* (Clouse et al., 1996; Friedrichsen et al., 2000), *bri1-3*, *bri1-4*, *bri1-5*, *bri1-6*, *bri1-7*, *bri1-8*, *bri1-9* (Noguchi et al., 1999), *bri1-5R1* (Belkhadir et al., 2010), *bri1-101*, *bri1-102*, *bri1-103/104*, *bri1-105-107*, *bri1-108-112*, *bri1-113*, *bri1-114/116*, *bri1-115*, *bri1-117/118*, *bri1-119* (Li and Chory, 1997; Friedrichsen et al., 2000), *bri1-120* (Shang et al., 2011), *bri1-201*, *bri1-202* (Domagalska et al., 2007), *bri1-301* (Xu et al., 2008), and *bri1-701* (Gou et al., 2012).

To exclude the possibility that the phenotypes are caused by mutations of other genes closely linked to *BRI1*, which are not easily segregated out by backcrossing, we crossed these mutants with a number of known *bri1* weak alleles. If the phenotype is caused by a mutation in a different gene, the F1 seedlings should show a wild-type phenotype due to functional complementation. All the obtained F1 seedlings show *bri1*-like phenotypes (Fig. 3A). In addition, we transformed the wild-type *BRI1* sequence driven by its native promoter into these nine different *bri1* mutant alleles. The transgenic plants showed *BRI1*-overexpressing phenotypes in the wild-type background (Fig. 3B; Wang et al., 2001; Nam and Li, 2002). We next transformed the genomic DNA sequences (containing the *BRI1* promoter and its coding sequences) of *bri1-702* and *bri1-705* to the null mutant, *bri1-701*. The resulting transgenic plants resembled the phenotypes of *bri1-702* and *bri1-705*, respectively (Fig. 3C). These genetic and transgenic results demonstrated that all nine new mutants are truly allelic to *bri1*.

Characterization of Newly Identified *bri1* Mutants

Root inhibition analysis indicated that *bri1-702* and *bri1-705* are less sensitive to exogenously applied BL (Fig. 4A). It is interesting that the rosette of *bri1-706* is significantly bigger than those of *bri1-702* and *bri1-705* (Fig. 2A), but its root growth is almost completely insensitive to BL treatment, similar to that of null *bri1* mutants (Fig. 4, A and D). *bri1-707*, *bri1-710*, and *bri1-711* show slightly reduced sensitivity to BL compared with Col-0 (Fig. 4B). All new *bri1* strong mutants, including *bri1-703*, *bri1-704*, *bri1-708*, and *bri1-709*, are insensitive to BL, similar to *bri1-701* (Fig. 4C; Gou et al., 2012). Previous studies indicated that *bri1* weak mutants show reduced sensitivity to BL but increased sensitivity to brassinazole (BRZ), a specific BR biosynthetic inhibitor (Asami et al., 2000; Yin et al., 2002). Therefore, we tested the sensitivity of these new *bri1* alleles to BRZ under darkness. As expected, the hypocotyl growth of weak and subtle alleles exhibited hypersensitivity to BRZ, whereas all strong alleles are

Table I. *bri1 alleles (for references, see Fig. 1)*

Allele	Base Pair Change	Accession	Allelic Strength	Possible Mechanism
bri1-1	G2725A	Col-0	Strong	Unknown
bri1-3	4-bp deletion after 2,745	Wassilewskija-2 (WS2)	Strong	Premature stop
bri1-4	10-bp deletion after 459	WS2	Strong	Premature stop
bri1-5	G206A	WS2	Weak	ER retention
bri1-5R1	G260A	*bri1-5*	Weak	Partially restore ER retention of *bri1-5*
bri1-6/119	G1931A	Enkheim-2 (En-2)	Weak	Unknown
bri1-7	G1838A	WS2	Weak	Unknown
bri1-8/108-112	G2948A	WS2/Col-0	Intermediate	Autophosphorylation cannot be detected in vitro
bri1-9	C1985T	WS2	Weak	ER retention
bri1-101	G3232A	Col-0	Strong	Autophosphorylation cannot be detected in vitro
bri1-102	C2249T	Col-0	Strong	Unknown
bri1-103/104	G3091A	Col-0	Strong	Unknown
bri1-105-107	C3175T	Col-0	Strong	Unknown
bri1-113	G1832A	Col-0	Strong	Unknown
bri1-114/116	C1747T	Col-0	Strong	Unknown
bri1-115	G3143A	Col-0	Strong	Unknown
bri1-117/118	G3415A	Col-0	Strong	Unknown
bri1-120	T1196C	Landsberg *erecta*	Weak	Unknown
bri1-201	G1831A	WS2	Strong	Unknown
bri1-202	C2854T	WS2	Strong	Unknown
bri1-301	GG2965/6AT	Col-0	Weak	Autophosphorylation of bri1-301 cannot be detected in vitro, but transphosphorylation of BAK1 can be detected in vivo
bri1-701	T-DNA insertion	Col-0	Strong	Knockout of *BRI1*
bri1-702	C3148T	Col-0	Weak	Reduced autophosphorylation in vitro
bri1-703	G3166A	Col-0	Strong	Autophosphorylation cannot be detected in vitro
bri1-704	G3079A	Col-0	Strong	Autophosphorylation cannot be detected in vitro
bri1-705	C2156T	Col-0	Subtle	Disrupt the formation of hydrogen bonds among BRI1, BL, and BAK1
bri1-706	C758T	Col-0	Subtle	Unknown
bri1-708	C2947G	Col-0	Strong	Autophosphorylation cannot be detected in vitro
bri1-709	G2543A	Col-0	Strong	Premature stop
bri1-710	G1858A	Col-0	Subtle	Unknown
bri1-711	G2236A	Col-0	Subtle	Unknown

insensitive to the BRZ treatment (Fig. 4E). These data indicated the new *bri1* alleles exhibit typical *bri1* phenotypes and reduced sensitivity to exogenously applied BL.

Previous studies also indicated that, upon application of exogenous BL, the expression of the BR biosynthesis gene *CPD* is down-regulated and the expression of a BR response gene, *SAUR-AC1*, is up-regulated (Li et al., 2001b; Yin et al., 2005). In addition, the phosphorylation status of BES1 also can be used as an indicator of a downstream signaling response to the BL treatment (Yin et al., 2002; Sun et al., 2010; Yu et al., 2011). Quantitative real-time PCR was performed to examine the expression levels of *CPD* and *SAUR-AC1* in the wild type and newly identified *bri1* mutants treated with or without 1 μM BL (Fig. 5, A and B). Similar to previous reports, the expression of *SAUR-AC1* was increased dramatically in Col-0 but had no significant change in *bri1-701* after the BL treatment. The expression of *SAUR-AC1* in the newly identified weak and subtle *bri1* alleles exhibited reduced sensitivity to the BL treatment, whereas in newly identified strong *bri1* alleles, the expression of *SAUR-AC1* is insensitive to treatment with BL and remained at a lower level of expression with or without the treatment (Fig. 5A). Similar to the *SAUR-AC1* response, the *CPD* responses of *bri1-702* and *bri1-705* showed reduced sensitivity to the BL treatment (Fig. 5B). Although the expression levels of *CPD* in BR-treated *bri1-706*, *bri1-707*, *bri1-710*, and *bri1-711* decreased relatively to the same degree compared with Col-0, basal expression levels of *CPD* without BL treatment were higher than in the wild type, suggesting that BR signaling is indeed partially altered in these mutants (Fig. 5B).

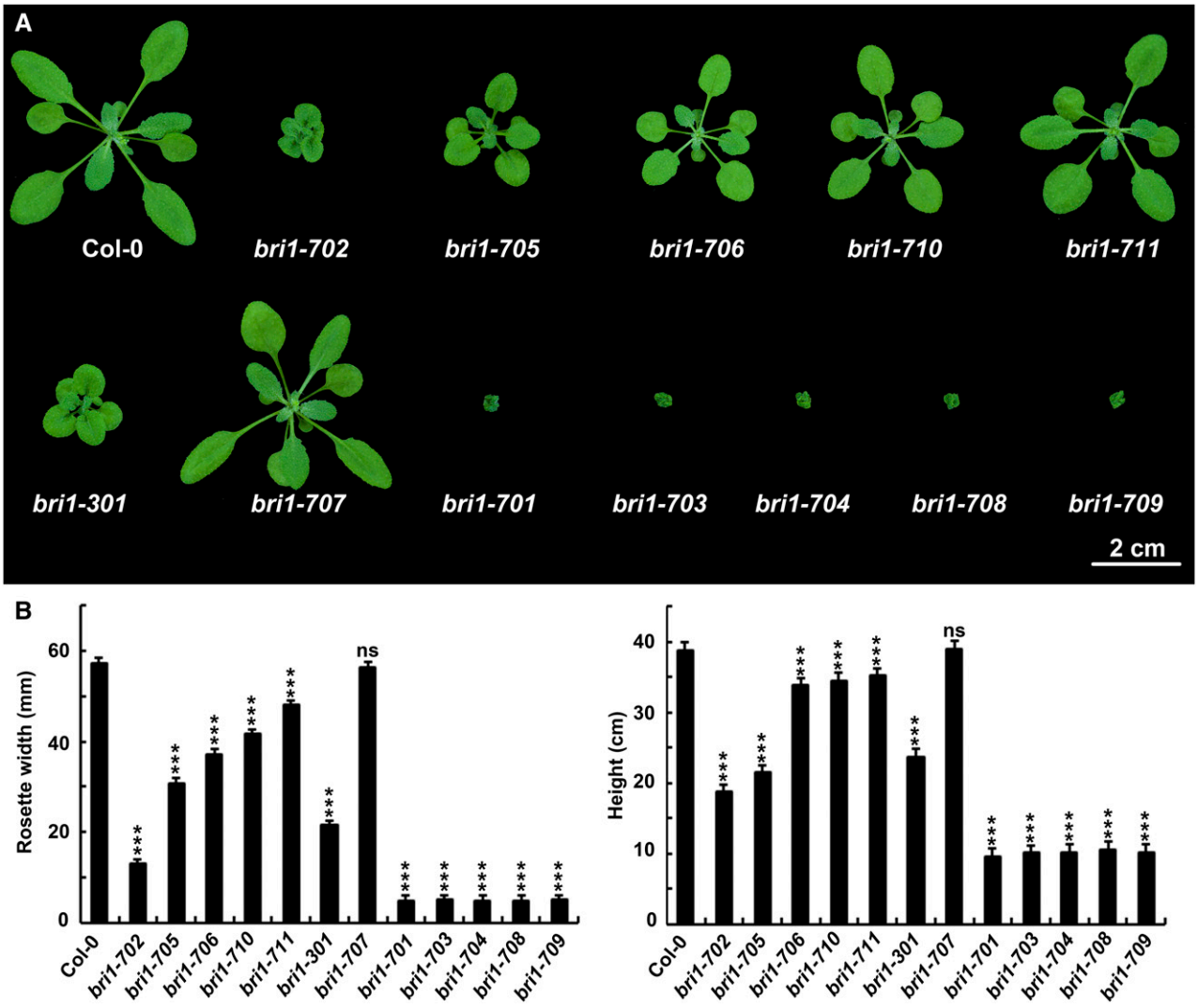

Figure 2. New *bri1* mutants identified in this study and their phenotypes. A, Phenotypes of mutants and wild-type seedlings. The photograph was taken 3 weeks after germination. B, Rosette width and height of the mutants and wild-type seedlings. Rosette width was measured 3 weeks after germination. Height was measured when growth was completely finished. Student's *t* tests were carried out to show the significance between each allele and Col-0. Each data point shown is the average and SD ($n \geq 20$). ***, $P < 0.001$; and ns, not significant.

We next investigated the phosphorylation status of BES1 in the wild type and in the newly identified *bri1* mutants with or without 1 μM BL application (Fig. 5, C and D). In Col-0, two almost equal intensity bands, representing phosphorylated and unphosphorylated forms of BES1, were detected without the BL treatment. After the BL treatment, phosphorylated BES1 was reduced greatly and unphosphorylated BES1 was accumulated significantly in Col-0, suggesting that the BR signaling pathway is functional. In *bri1-702* and *bri1-705*, only a small amount of unphosphorylated BES1 was detected after the BL treatment. In the strong *bri1* alleles *bri1-701*, *bri1-703*, *bri1-704*, *bri1-708*, and *bri1-709*, the accumulation of unphosphorylated BES1 could not be easily observed after the treatment with BL. In subtle alleles, *bri1-711*, *bri1-710*, and *bri1-706*, the accumulation of unphosphorylated BES1 is similar to that in Col-0 upon treatment with 1 μM BL. It is intriguing that *bri1-301* and *bri1-707* contain different missense mutations at the same residue, but the BES1 response to BL is totally different. *bri1-301* remains partially sensitive, while *bri1-707* is completely sensitive to the treatment with BL (Fig. 5, C and D). These molecular and biochemical results confirmed that *bri1-706*, *bri1-710*, and *bri1-711* are subtle alleles of *bri1*.

bri1-702, with a Point Mutation in the Activation Loop of BRI1, Shows Reduced Autophosphorylation Activity

Autophosphorylation, especially the pocket opening of the activation loop, is a common activation mechanism for

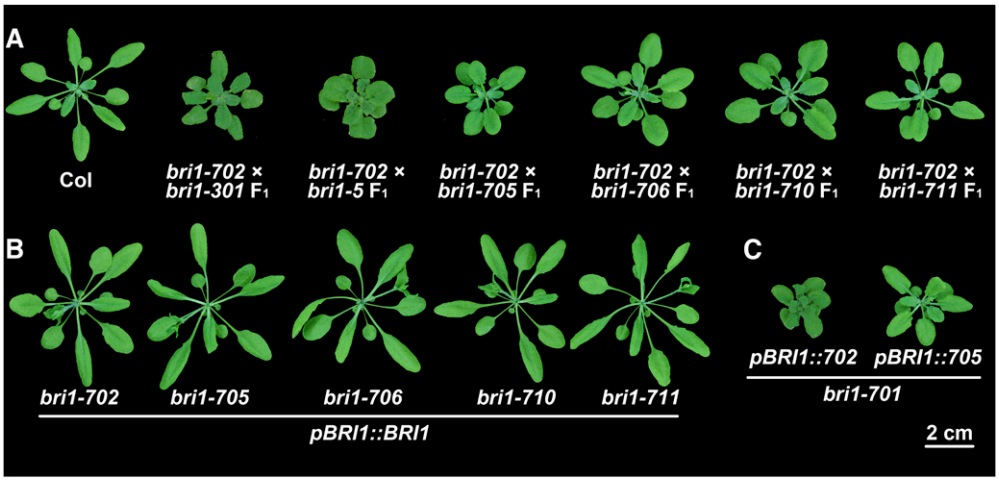

Figure 3. Complementation analyses confirm that all mutants are alleles of *bri1*. A, The phenotypes of new *bri1* weak or subtle alleles cannot be complemented by other *bri1* weak alleles. B, *BRI1* driven by its native promoter can completely rescue the phenotypes of new *bri1* weak or subtle alleles. C, The phenotypes of *bri1-702* and *bri1-705* can be recapitulated by expressing their corresponding genomic DNA in a null *BRI1* mutant allele, *bri1-701*. Photographs were taken 4 weeks after germination.

protein kinases (Oh et al., 2000). In order to understand whether the mutations in the newly identified *bri1* mutants affect the kinase activity of BRI1, we used the phospho-amino acid stain Pro-Q Diamond to detect the autophosphorylation activity of the *Escherichia coli*-expressed mutant BRI1 cytoplasmic domain (CD) fused with a maltose-binding protein (MBP-BRI1-CD; Fig. 6, A and B). After sequential staining with the Pro-Q Diamond and Coomassie Blue Silver, the *E. coli* cell lysate, which contains the expressed bri1-301-CD, exhibited an undetectable kinase activity in vitro, similar to the results from a previous report (Xu et al., 2008). However, bri1-707-CD, which bears a different substitution at the same residue with bri1-301-CD, showed reduced but detectable autophosphorylation activity (Fig. 6, A and B). Interestingly, compared with the undetectable kinase activities of other intracellular *bri1* mutants, *bri1-702*, a weak allele with a mutation in the activation loop, still shows autophosphorylation activity, although it is partially reduced compared with the wild type (Fig. 6, A and B). This result indicated that mutation of *bri1-702* leads to a reduced kinase activity of BRI1 and, therefore, attenuated BR signal transduction.

To confirm these results in vivo, we generated transgenic plants overexpressing *BAK1-GFP* in Col-0 and various genotypic backgrounds. A phospho-Thr antibody was used to detect the phosphorylation on Thr residues of immunoprecipitated BAK1-GFP from different backgrounds applied with or without BL (Fig. 6C). Similar to a previous report (Wang et al., 2008), the phosphorylation level of BAK1 was strongly enhanced by the BL treatment or by overexpressing *BRI1* in Col-0. The phosphorylation of BAK1 was reduced to an almost undetectable level and exhibited no response to BL treatment in *bri1* null alleles. In *bri1-702* and *bri1-301*, the phosphorylation level of BAK1 was induced slightly by exogenously applied BL. Interestingly, without BL, the phosphorylation level of BAK1 was much higher in these two weak alleles than even in the wild type (Fig. 6C). These results suggested that *bri1-702*, the only weak allele in the activation loop identified so far, exhibited not only a reduced autophosphorylation activity of BRI1 in vitro but also a reduced sensitivity of the BAK1 phosphorylation response to exogenously applied BL in vivo. Even though in vitro bri1-301 autophosphorylation could not be detected, as reported previously (Xu et al., 2008), BAK1 phosphorylation in the *bri1-301* background is much higher than that in *bri1-701* and is induced by the addition of BL. This result suggests that bri1-301 is indeed partially functional toward its substrate in vivo, clarifying a previous argument regarding whether the kinase activity of BRI1 is even critical to the BR signaling transduction (Xu et al., 2008).

Overexpression of *mBAK1* Failed to Generate a Dominant Negative Phenotype in *bri1-705*

Structural analysis suggested that the extracellular portions of BRI1 and BAK1 can form a BL-induced complex (Santiago et al., 2013; Sun et al., 2013). Several crucial surfaces for the interaction of BRI1 and BAK1 also were identified, among which were two residues of BRI1 (Thr-726 and Met-727) associated directly with BAK1 via hydrophobic interactions (Santiago et al., 2013; Sun et al., 2013). Coincidentally, *bri1-705*, a new subtle allele with a typical BR-deficient phenotype, contained a nearby mutation at Pro-719 to Leu, which may affect the interaction between BRI1 and BAK1. In order to test this hypothesis, a series of transgenic analyses were carried out. Based on previous studies, overexpression of *BAK1* can suppress the phenotype of

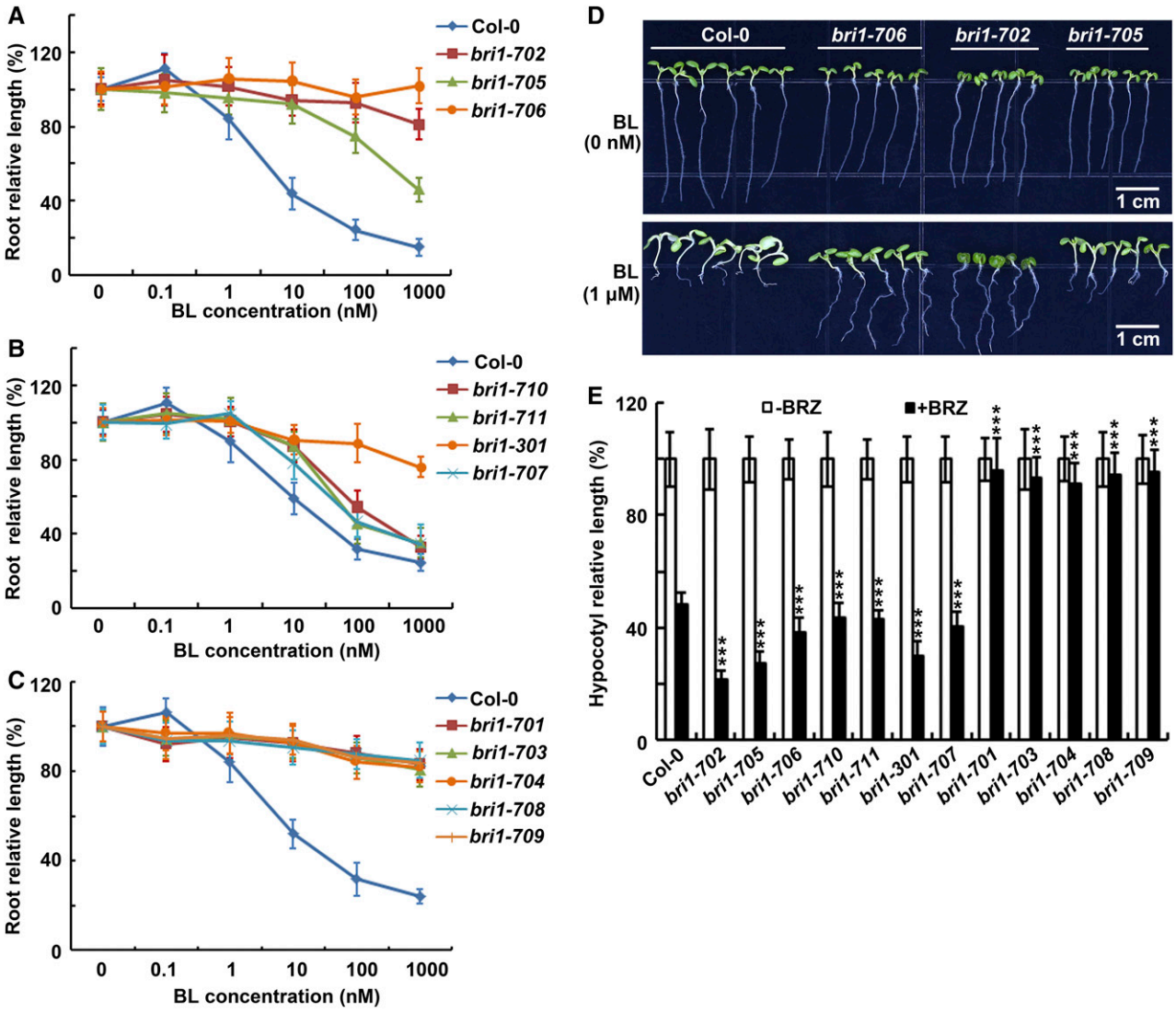

Figure 4. All mutants show either insensitivity or reduced sensitivity to exogenously applied BL. A to C, Responses of root growth to treatment with BL. Seven-day-old seedlings were grown on one-half-strength Murashige and Skoog (MS) medium supplemented with different concentrations of BL. D, *bri1-706* is almost completely insensitive to BL. Seven-day-old seedlings were grown on one-half-strength MS medium supplemented with or without 1 μM BL. The seedlings were grown under long-day light conditions in a 22°C growth chamber for A to D. E, Responses of hypocotyl growth to treatment with BRZ. Four-day-old seedlings were grown on one-half-strength MS medium with or without BRZ application under darkness in a 22°C growth chamber. Student's *t* tests were performed to show significance between each allele and Col-0. Each data point represents the average and SD ($n \geq 20$). ***, $P < 0.001$.

bri1-5, while overexpression of a kinase-inactive version of BAK1 (*mBAK1*), in which a point mutation is introduced on a conserved Lys residue within the ATP-binding site, results in a dominant negative phenotype (Li et al., 2002; Gou et al., 2012). Both genetic suppression and dominant negative phenotypes rely on interactions between the extracellular portion of BRI1 and BAK1. If a mutation in BRI1 disrupts the interaction with BAK1 or mBAK1, overexpression of *mBAK1* may not dramatically alter the phenotype of the *bri1* mutant. *BAK1-GFP* and *mBAK1-GFP* were transformed to a series of weak *bri1* alleles. Consistent with previous reports (Li et al., 2002), the defective phenotype of *bri1-5* was partially rescued by overexpressing *BAK1* but greatly enhanced by overexpressing *mBAK1* (Supplemental Fig. S2). Overexpression of *BAK1* or *mBAK1* in *bri1-301* and *bri1-702* resulted in phenotypes similar to those in *bri1-5* (Fig. 7; Li et al., 2002). However, overexpression of *BAK1* or *mBAK1* failed to dramatically alter the phenotype of *bri1-705* (Fig. 7), suggesting that the mutation in *bri1-705* may interfere with the interaction between bri1-705 and BAK1 or mBAK1. These genetic data demonstrated that the BL-dependent extracellular heterodimerization of BRI1 and BAK1 is an important step in the initiation of BR signaling.

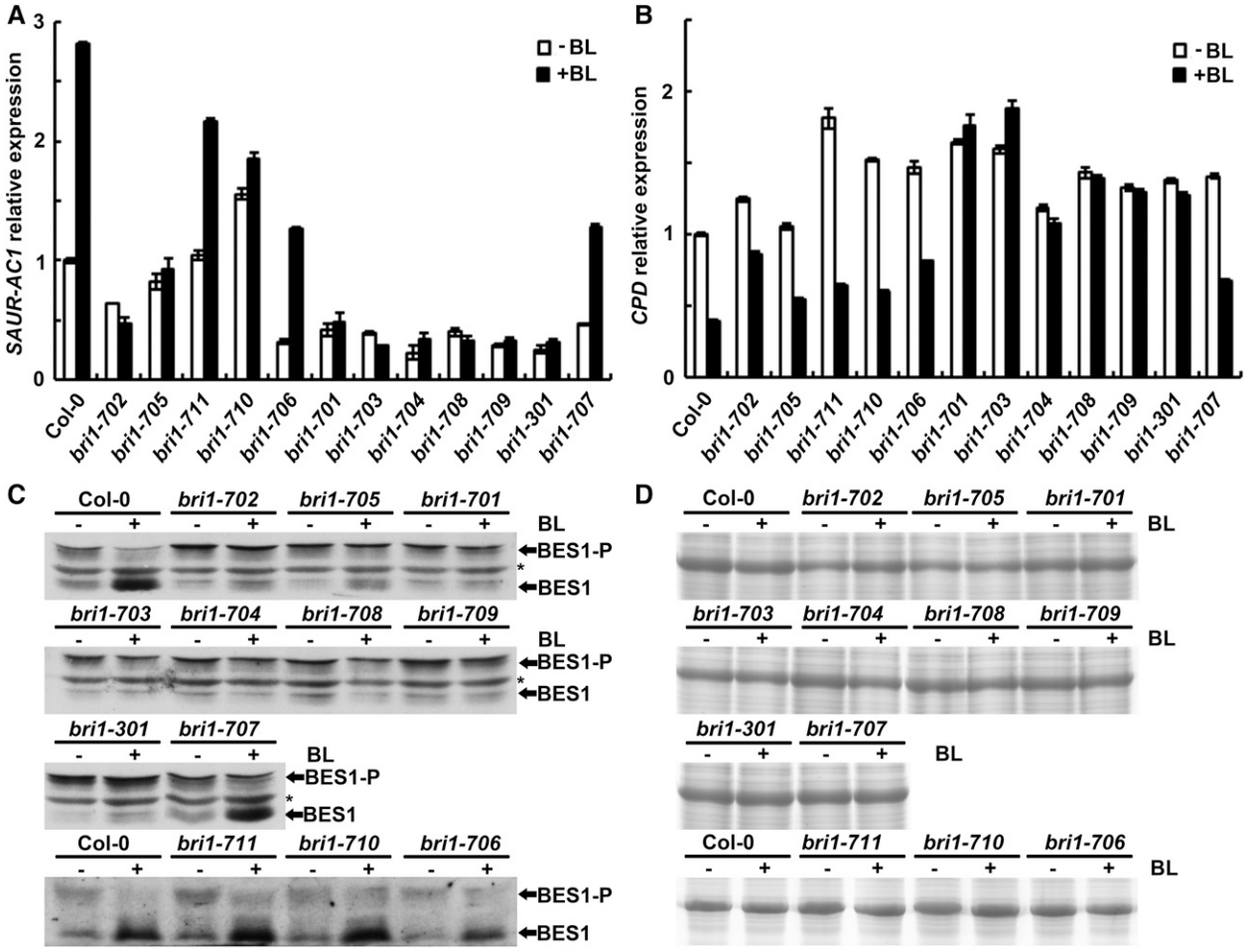

Figure 5. Responses of downstream BR signaling components of the new mutants to BL. A and B, Transcriptional responses of *SAUR-AC1* and *CPD* to treatment with BL. *ACTIN2* was used as a reference gene. Error bars represent SD ($n = 3$). C, Responses of BES1 phosphorylation status to treatment with BL. Total protein was extracted and immunoblotted with an anti-BES1 antibody. D, Coomassie Blue staining showing equal loading between each pair of samples in C. Seven-day-old long-day-grown seedlings treated with or without 1 μM BL for 4 h were used. −, Without BL treatment; +, with BL treatment; *, nonspecific band. BES1-P, Phosphorylated BES1; BES1, unphosphorylated BES1.

To further confirm this notion, we performed a molecular dynamic (MD) simulation analysis of the BRI1-BL-BAK1 structure. The fluctuation of 120-ns MD trajectories obtained from two simulation systems (the wild-type complex and the BRI1-Pro-719Leu complex) was monitored using the root mean square deviation of the backbone atoms of BRI1, BAK1, and BL (Supplemental Fig. S3). It can be seen clearly that the root mean square deviation values of both BRI1-Pro-719Leu and wild-type BRI1 oscillate at ~4 Å after 20 ns, whereas the structural fluctuations of BAK1 and BL are significantly higher in the BRI1-Pro-719Leu complex compared with the wild-type complex, implying that the Pro-719Leu mutation of BRI1 may destabilize the interactions of BRI1-BL and BRI1-BAK1. The simulation analysis also showed that the mutation leads to significant conformation alterations of Arg-717, which precedes Pro-719 and has the propensity to change from a random coil to a β-turn in the mutant complex. Meanwhile, the β-turn structure formed by Asn-705 and Ile-706 in the wild-type complex seems to be destabilized and prone to show a random coil conformation in the mutant complex (Fig. 8A). Analysis of the interaction interfaces revealed that the hydrogen bonding of the residue Asn-705, which bridges the side chain of His-61 from BAK1 and the hydroxyl group of BL, was interrupted continuously in the BRI1-Pro-719Leu complex during the last 20-ns simulation (Fig. 8B). Additionally, the hydrogen bond between the main-chain oxygen atom of His-61 from BAK1 and the hydroxyl group of BL also breaks up more frequently in the BRI1-Pro-719Leu complex compared with the wild-type complex (Fig. 8B). Taken together, these results suggest that the mutation in *bri1-705* results in significant local conformational changes involving the residue Asn-705 that interacts with both BAK1 and BL, thus

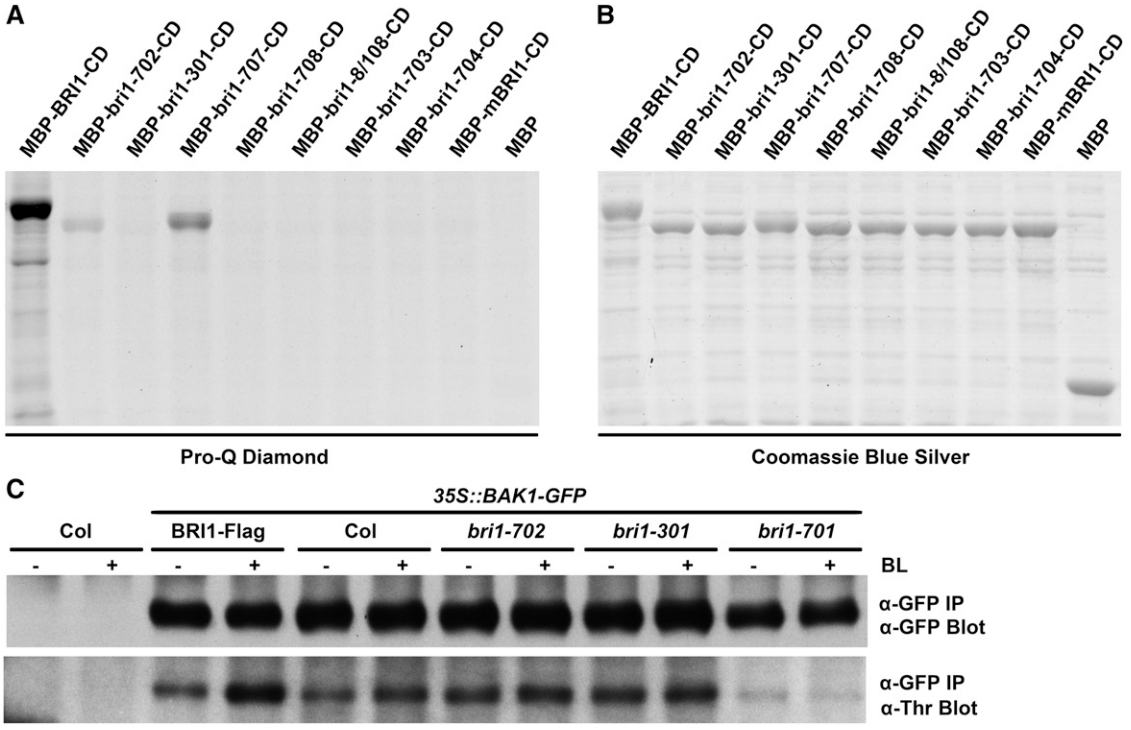

Figure 6. In vitro and in vivo phosphorylation analyses of BRI1, bri1, and BAK1. A, Pro-Q Diamond analyses of BRI1 and various bri1 cytoplasmic domains. The recombinant proteins were expressed in *E. coli*, and total protein extracts were separated by 10% SDS-PAGE. The gel was stained by Pro-Q Diamond. B, Coomassie Blue Silver staining to show equal loading of the samples. mBRI1 contains a mutation within the ATP-binding site (Lys-911Glu). C, In vivo phosphorylation analyses of BAK1-GFP from various *bri1* mutants in response to treatment with BL. Membrane proteins were extracted from 10-d-old long-day-grown seedlings treated with or without 100 nM BL for 1.5 h. BAK1-GFP proteins from different *bri1* alleles were immunoprecipitated (IP) with an anti-GFP antibody. The phosphorylation levels of BAK1 were detected with a phospho-Thr antibody. The immunoprecipitated BAK1-GFP was immunoblotted with an anti-GFP antibody to show equal loading. −, Without BL treatment; +, with BL treatment.

destabilizing the pairwise interactions among BRI1, BAK1, and BL (Fig. 8C).

bri1 Point Mutants Exhibiting Defective Phenotypes All Bear Point Mutations within Conserved Residues among BRI1s and BRLs

Eighty-three missense mutations of *BRI1* were isolated in this study, among which nine point mutations resulted in typical *bri1* phenotypes, including one mutation that generated a premature stop codon, and 74 point mutations did not show any significant phenotypes in normal laboratory growing conditions. There were 16 different *bri1* point mutants identified in previous reports (premature stop mutants are not included). Altogether, 98 point mutations of BRI1 have been found so far. We were curious whether these 24 *bri1* point mutants (16 previously identified plus eight newly identified) with mutant phenotypes all contain point mutations in conserved residues. We thus carried out a sequence alignment among 70 BRI1s or BRLs from 18 sequenced flowering plant species (Fig. 9A). As expected, all of these mutants are mutated at conserved residues, but their phenotypes are not positively related to the degree of conservation. Surprisingly, not all mutations of conserved residues exhibit defective phenotypes (Fig. 9A). As BRI1 is a typical LRR-RLK with multiple functional domains, we also performed sequence analysis among all LRR-RLKs from Arabidopsis (Fig. 9B). These results indicated that not all mutation residues of 24 *bri1* mutants are conserved among all LRR-RLKs. These residues may be particularly important for specific BRI1 functions that have been evolutionarily selected. We also found that not all mutations of conserved residues among all LRR-RLKs exhibit defective phenotypes (Fig. 9B).

DISCUSSION

The activation loop is a crucial region for protein kinase activity (Oh et al., 2000). Sequence analysis indicated that most residues in the activation loop are extremely conserved in 70 BRI1s/BRLs obtained from 18 sequenced flowering plant species (Supplemental Fig. S4A). Besides, there are several residues in the activation loop of BRI1 that also are conserved in all Arabidopsis LRR-RLKs (Supplemental Fig. S4B). Two

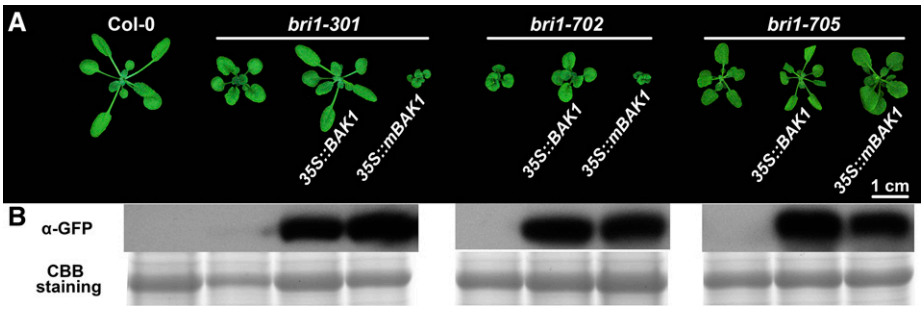

Figure 7. Overexpression of *mBAK1* in *bri1-301* and *bri1-702* but not in *bri1-705* resulted in dominant negative phenotypes. A, Phenotypes of the transgenic plants and their backgrounds. The photograph was taken 3 weeks after germination. B, Western-blot analyses showing the expressed BAK1-GFP and mBAK1-GFP fusion proteins in transgenic plants. Total proteins from rosette leaves were extracted and immunoblotted with an anti-GFP antibody. mBAK1 contains a mutation within the ATP-binding site (Lys-317Glu). CBB, Coomassie Blue Silver.

new *bri1* strong alleles, *bri1-703* and *bri1-704*, contain mutations in the last and first residues of the BRI1 activation loop, respectively, and both of them are extremely conserved not only in BRI1s or BRLs but also in all other Arabidopsis LRR-RLKs. Two previously reported alleles, *bri1-103/104* and *bri1-115*, with mutations on extremely conserved residues among BRI1s or BRLs but less conserved among all other LRR-RLKs, also show strong *bri1* phenotypes (Supplemental Fig. S4; Li and Chory, 1997; Friedrichsen et al., 2000). We found that *bri1-702*, the only weak allele in the activation loop of BRI1, contains a mutation in Pro-1050 that is extremely conserved in BRI1s or BRLs but not conserved in all other LRR-RLKs (Supplemental Fig. S4). However, there also is a mutation found via TILLING in Arg-1032Lys that has the same degree of conservation with *bri1-103/104* among BRI1s or BRLs but showed no defective phenotypes, possibly because it is mutated to Lys, which shows a similar degree of conservation with Arg in other LRR-RLKs (Supplemental Fig. S4). Among all Arabidopsis LRR-RLKs, several residues mutated in *bri1* alleles are not even conserved. We suggest that these mutation residues may be related to the specificity of the BRI1-mediated signaling pathway (Fig. 9B).

In previous studies, the importance of the BRI1 kinase activity was questioned because bri1-301-KD showed no kinase activity in vitro, either via an autophosphorylation assay or an analysis of its phosphorylation activity toward BAK1, but exhibits a weak *bri1* phenotype (Xu et al., 2008). In our studies, the bri1-301-CD fusion protein extracted from *E. coli* also could not be stained by the phosphoprotein Pro-Q Diamond (Fig. 6, A and B). However, we noticed that, unlike in a *bri1* null allele, the BAK1 phosphorylation level in *bri1-301* is even higher than that of the wild type as detected by immunoblotting using a phospho-Thr antibody (Fig. 6C). This is possibly caused by higher endogenous levels of BL in *bri1-301*, as was found in other *bri1* mutants (Noguchi et al., 1999). The phosphorylation level of BAK1 in *bri1-301* can be induced significantly by BL in vivo (Fig. 6C). This result indicated that bri1-301-CD possesses kinase activity for its substrate BAK1 in vivo. The undetectable autophosphorylation of bri1-301-CD in vitro may be caused by protein misfolding when expressed in *E. coli*.

In this study, we also have some interesting findings from analyzing new *bri1* mutant alleles. For example, *bri1-707* (Gly-989Glu, Col-0 accession) contains the same mutation as *bri1-301* (Gly-989Ile, Col-0 accession), but with a different amino acid substitution. As a result, *bri1-707* shows a wild-type-like phenotype (Fig. 2). Actually, the change of Gly to Glu is predicted to substitute a larger side chain than Gly to Ile because of an additional carboxyl group in Glu. Similarly, the new strong allele *bri1-708* (Arg-983Gly, Col-0 accession) also bears a point mutation at the same residue as *bri1-8* (Arg-983Gln, WS2 accession) and *bri1-108-112* (Arg-983Gln, Col-0 accession). However, the Arg-to-Gly substitution causes a greater phenotypical alteration than the Arg-to-Gln substitution. These results indicated that the mechanisms of point mutation are complicated and may involve structural changes.

We identified an extracellular subtle mutant, *bri1-705*, which has an amino acid substitution close to the BRI1-BAK1 interaction surface. Unlike other weak alleles, such as *bri1-5*, *bri1-702*, and *bri1-301*, overexpression of *mBAK1* in *bri1-705* failed to generate a dominant negative phenotype (Fig. 7). This result suggested that the mutation in *bri1-705* may affect the interaction between the extracellular portions of BRI1 and BAK1. This is further supported by the MD simulation results, indicating that the mutation in *bri1-705* results in significant local conformational changes, causing the disruption of three pairs of hydrogen bonds formed between BRI1-Asn-705 and BAK1-His-61, BRI1-Asn-705 and BL, and BAK1-His-61 and BL. Alterations of this hydrogen bonding network could potentially destabilize the pairwise interactions among BRI1, BAK1, and BL and lead to decreased binding affinity of the BRI1-BAK1 extracellular portions. Our data, therefore, provide additional genetic and structural evidence for the crucial role of BL-dependent BRI1-BAK1 heterodimerization in the early events of BR signaling.

During our study, we identified another surprising *bri1* mutant, *bri1-706*. *bri1-706* only shows a subtle

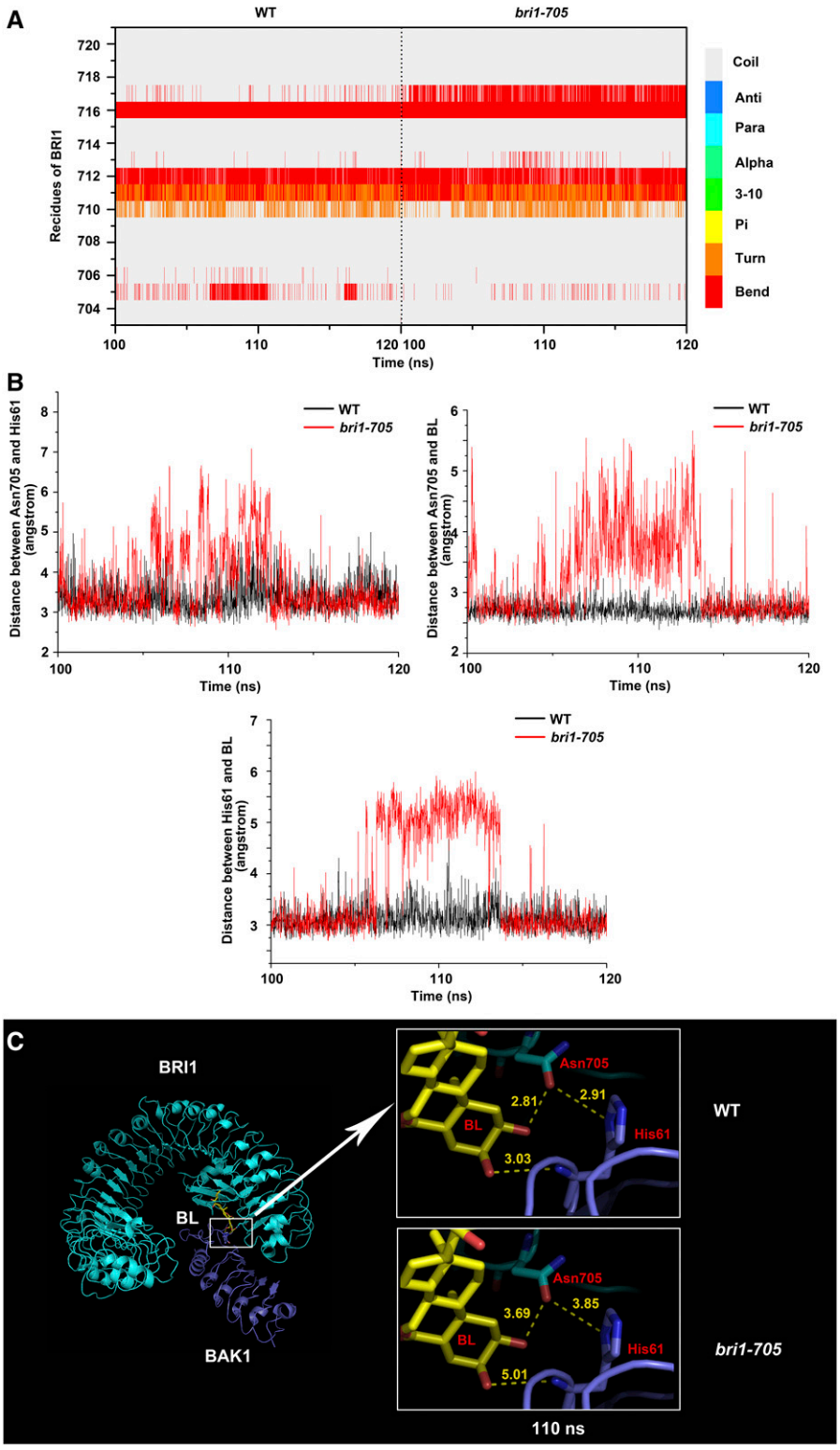

Figure 8. Conformational changes monitored during the last 20-ns MD simulation. A, Time evolution of the secondary structures of residues 703 to 721 of BRI1 in the wild-type (WT) complex (left) and the mutant complex (right). Compared with the wild-type complex, the residue Arg-717 preceding Pro-719 has the propensity to change from a random coil to a β-turn, while Asn-705 and Ile-706 seem to be destabilized and prone to adopt a random coil conformation in the mutant complex. B, Monitoring time evolution of the distances between the atom OD1 of BRI1-Asn 705 and ND1 of BAK1-His-61 (top left), atom OD1 of BRI1-Asn-705 and O02 from C2 of BL (top right), and atom ND1 of BAK1-His-61 and O03 from C3 of BL (bottom). The distances in the wild-type complex and the mutant complex are colored in black and red, respectively. C, Interaction modes of BRI1-Asn-705 (cyan), BAK1-His-61 (purple), and BL (yellow). At 110 ns, as shown in the top right inset, Asn-705, His-61, and BL form pairwise hydrogen bonds, indicated by the close distances of 2.91, 2.81, and 3.03 Å between Asn-705, His-61, and BL, respectively. However, in the bri1-705 mutant complex, as shown in the bottom right inset, these hydrogen bonds are disrupted, as evidenced by the much larger pairwise distances between Asn-705, His-61, and BL.

morphological phenotype compared with other weak alleles isolated so far (Fig. 2). However, root inhibition and hypocotyl promotion assays showed that *bri1-706* is greatly insensitive to treatment with BL (Fig. 4A; Supplemental Fig. S5A). When *pBRI1*::*BRI1* was introduced in *bri1-706*, both the phenotype and insensitivity to BL were completely restored (Fig. 3B; Supplemental Fig. S5B). Endo H analyses indicated that bri1-706 proteins are partially retained in ER in 10-d-old seedlings, in which roots and shoots of the seedlings showed no significant differences

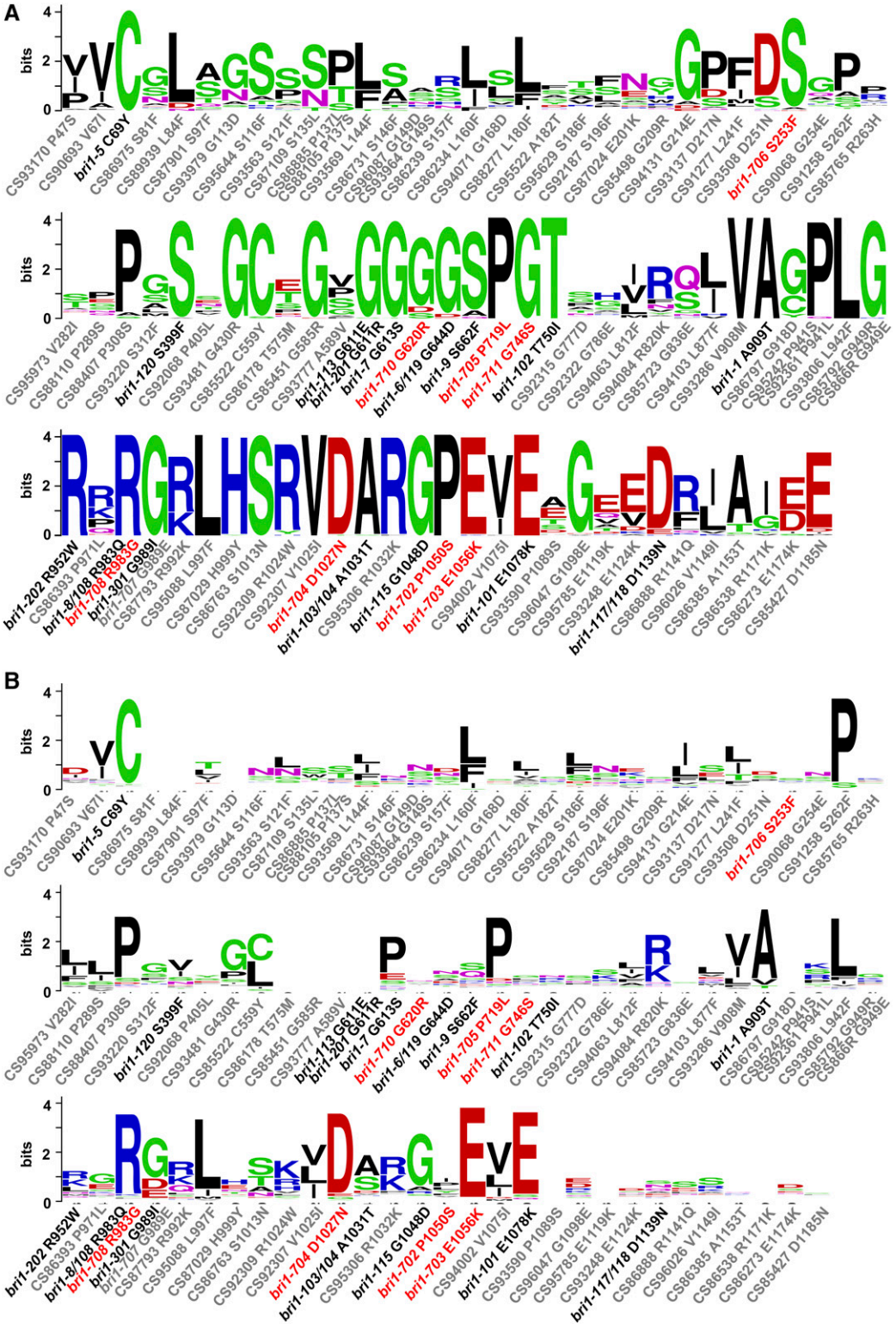

Figure 9. Sequence analyses of all 98 BRI1 point mutations. A, Sequence analyses among 70 BRI1s or BRLs from 18 sequenced flowering plant species. Mutants showing defective phenotypes all result from mutations of conserved residues. But not all mutations in the conserved residues show defective phenotypes. B, Sequence analyses among all 223 LRR-RLKs of Arabidopsis. Not all mutation sites from mutants with defective phenotypes are conserved, and vice versa. Only the amino acid sites with mutations are shown. New mutants from this study are labeled in red. Previously known mutants are labeled in black. New mutations without significant phenotypes are labeled in gray. The size of the logo is positively correlated to the degree of conservation.

(Supplemental Figs. S5, C and D, and S6). But *CPD* down-regulation and unphosphorylated BES1 accumulation in response to exogenous BL in *bri1-706* are similar to those of wild-type seedlings (Supplemental Fig. S5, E–G). To our knowledge, this is the first *bri1* mutant showing that phenotypic severity is not positively correlated with the degree of insensitivity to exogenous BL application. These data suggest that the specific mutation found in *bri1-706* may have destroyed the interaction of bri1-706 with an unknown protein that may regulate a branch of the BR signaling pathway. Detailed molecular mechanisms regarding how *bri1-706* affects root growth sensitivity to BL need to be investigated further in the near future.

We identified a strong allele, *bri1-709*, in which a point mutation results in a premature stop codon within the juxtamembrane region (Supplemental Fig. S7A). Interestingly, a specific band that is smaller than that in Col-0 can be detected by an immunoblot assay using total proteins from *bri1-709* plants with an anti-BRI1 antibody (Supplemental Fig. S7B). This result suggests that the early stop codon of *bri1-709* did not disrupt the protein transport of BRI1 and that a partial BRI1 protein without the kinase domain and the C terminus is expressed in *bri1-709*. This mutant can be used for future genetic and biochemical analyses.

In previous studies, two extracellular weak alleles, *bri1-5* and *bri1-9*, were found to be retained in the ER, because the mutational BRI1 proteins interact with ER chaperones and fail to pass the ER quality control system (Jin et al., 2007, 2009; Hong et al., 2008). In order to test whether BRI1 is retained in the ER for our newly identified extracellular mutation alleles, we performed an Endo H analysis (Supplemental Fig. S6). The results indicated that BRI1 is not retained on ER in *bri1-710* and *bri1-711* and is partially retained on ER in *bri1-705* and *bri1-706*. In *bri1-705* and *bri1-706*, there is still a considerable amount of BRI1 that is resistant to Endo H cleavage, suggesting that partially retained bri1-705 or bri1-706 on ER may not be the main reason for their defective phenotypes.

CONCLUSION

In this study, we analyzed 83 *BRI1* point mutations generated by TILLING, among which nine mutants showed typical *bri1* mutant phenotypes. *bri1-702* is a weak allele. *bri1-705*, *bri1-706*, *bri1-710*, and *bri1-711* are subtle alleles. *bri1-703*, *bri1-704*, *bri1-708*, and *bri1-709* are strong alleles, similar to *bri1-701* (Fig. 1; Table I). *bri1-702*, the first weak allele in the activation loop of BRI1 identified so far, exhibited not only reduced autophosphorylation activity of BRI1 in vitro but also reduced sensitivity of the BAK1 phosphorylation response to exogenously applied BL in vivo (Fig. 6). *bri1-705*, a new subtle allele in the extracellular portion, contains a BRI1 mutation that may disrupt the formation of hydrogen bonds among BRI1, BL, and BAK1 (Fig. 8). Surprisingly, *bri1-706*, a subtle morphological mutant with a mutation in the extracellular portion of BRI1, showed insensitive root growth inhibition to exogenously applied BL, which is similar to the null *bri1* mutants (Figs. 2A and 4A). The identification of unexpected characteristics of *bri1-706* suggests that there are still many unknown aspects in the early events of the BR signaling pathway waiting to be elucidated in the future.

MATERIALS AND METHODS

Plant Materials, Growth Conditions, and Mutant Detection

Original Arabidopsis (*Arabidopsis thaliana*) *bri1* TILLING seeds obtained from the Arabidopsis Biological Resource Center are all in the Col-0 accession, which contains an *er* mutation. After *er* and additional mutations were segregated out via backcrossing for at least three generations, each homozygous *bri1* was isolated and used for phenotypic determination and detailed analyses. Other known *bri1* mutants used in this study include *bri1-5* (WS2 background), *bri1-9* (Col-0 background), *bri1-301* (Col-0 background), and *bri1-701* (SALK_116202). All plants were grown in a greenhouse under a long-day lighting condition (16 h of light and 8 h of dark) or under darkness at 22°C. Seedlings were grown on one-half-strength MS agar plates or in liquid medium supplemented with 1% (w/v) Suc.

The dCAPS approach was used to confirm the point mutations (Neff et al., 1998). dCAPS Finder 2.0 (http://helix.wustl.edu/dcaps/dcaps.html) was used to design mismatched PCR primers to generate or disrupt a restriction enzyme recognition site relative to the mutation (Neff et al., 2002). All primers and enzymes used in this study for genotyping *bri1* TILLING mutations are listed in Supplemental Table S1.

Root Inhibition and Hypocotyl Growth Assays

Seeds were surface sterilized with 75% (w/v) ethanol for 30 s, followed by 1% NaClO for an additional 7 min, and washed with desterilized water five times. The seeds were then placed on one-half-strength MS plates with 0.8% (w/v) agar, 1% (w/v) Suc, and different concentrations of 24-epibrassinolide (Sigma) or BRZ (Santa Cruz Biotechnology). The seeds were vernalized at 4°C for 3 d and transferred to different growth conditions as indicated in the figure legends. Before being placed in the dark, plates were exposed to white light for 6 h to induce germination. All measurements were carried out using ImageJ (http://rsb.info.nih.gov/ij/).

Vector Construction and Transgenic Plant Generation

Gateway technology (Invitrogen, Life Technologies) was used in cloning all genes into expression vectors in this study. The full-length coding sequence fragments of *BRI1*, *BRI1-CD*, and *BAK1* were amplified and cloned into a *pDONR/Zeo* entry clone vector. Site-directed mutagenesis was carried out to generate mutated entry clones of *BRI1*, *BRI1-CD*, and *BAK1* based on the method described previously (Gou et al., 2012). All the cloned genes were sequence verified. Genes in the entry clone vectors were then cloned into various destination vectors for different purposes, such as *pBRI1-GWR-Flag*, *pBIB-BASTA-35s-GWR-Flag*, and *pBIB-HYG-35s-GWR-GFP*. All expression constructs were transferred into appropriate plant materials by the floral dip method (Clough and Bent, 1998).

RNA Extraction and Quantitative Real-Time PCR

Seven-day-old seedlings of Col-0 and *bri1* mutants grown on one-half-strength MS plates were collected and then grown with or without 1 μM 24-epibrassinolide in liquid medium for 4 h. Total RNAs were extracted using an RNA simple total RNA kit (Tiangen) and reverse transcribed to total cDNAs utilizing Moloney murine leukemia virus reverse transcriptase (Invitrogen, Life Technologies). Quantitative real-time PCR was performed by the StepOnePlus Real-Time PCR System (Applied Biosystems) utilizing SYBR Green reagent (Takara). Detailed experimental procedures were the same as reported previously (Zhao et al., 2016).

Membrane Protein Isolation, Immunoprecipitation, Western Blotting, and Phosphoprotein Staining

Ten-day-old seedlings of *35S::BAK1-GFP*, *35S::BRI1-FLAG*, Col-0 *35S::BAK1-GFP*, *bri1-702 35S::BAK1-GFP*, *bri1-301 35S::BAK1-GFP*, or *bri1-701 35S::BAK1-GFP* were treated with or without 100 nM 24-epibrassinolide for 1.5 h and then ground to a fine powder in liquid N_2. The membrane protein isolation procedure was the same as reported previously (Li et al., 2002). The soluble protein samples were immunoprecipitated utilizing an anti-GFP antibody (Invitrogen) combined with Protein A/G Plus-Sefinose Resin (BBI). The immunoprecipitated proteins were separated by 10% SDS-PAGE and tested by western analyses with anti-GFP and anti-phospho-Thr antibodies.

The same plant materials used for quantitative real-time PCR also were used in the detection of BES1 phosphorylation status. Total proteins were separated by 12% SDS-PAGE and detected via a specific anti-BES1 antibody (made by J.L.'s laboratory). The transgenic plants in Figure 7 were identified by detecting their GFP tag utilizing an anti-GFP antibody (Invitrogen). The Endo H analyses shown in Supplemental Figures S5 and S6 were performed as described previously (Hong et al., 2008). The total proteins of wild-type and mutant plants in Supplemental Figure S7 were separated by 8% SDS-PAGE and detected via a specific anti-BRI1 antibody (Agrisera; A177246). Horseradish peroxidase-linked anti-rabbit or anti-mouse antibody was used as a secondary antibody, and the signal was detected by Western Lightning Chemiluminescence Reagent Plus (Perkin-Elmer) in all western-blot experiments.

For the phosphoprotein staining assay, the cytoplasmic domain sequences of wild-type *BRI1* and mutated *BRI1* (residues 815–1,196) were cloned into the expression vector *pMAL-cRI-MBP-GWR*. The recombinant proteins were expressed in *Escherichia coli* and induced by 0.1 mM isopropylthio-β-galactoside for 6 h at 18°C. The cell lysates were boiled and centrifuged. The supernatant was separated by 10% SDS-PAGE and stained sequentially with Pro-Q Diamond (Invitrogen) and Coomassie Blue Silver as described previously (Taylor et al., 2013).

MD Simulation Analysis

The initial complex coordinates of BRI1-BAK1-BL were retrieved from the Protein Data Bank (http://www.rcsb.org) under accession code 4M7E (Sun et al., 2013). MD simulations were carried out using the AMBER 10 software package (Case et al., 2005) to check the stability of BRI1 and BAK1 in complex with BL. We used the AMBER ff12SB (Hornak et al., 2006) force field for the protein and water and the general AMBER force field (Wang et al., 2004) for the BL molecule. Atom types and AM1-BCC atomic charges were generated for BL using the Antechamber module. The LEaP module of the AMBER 10 software package was used to prepare the protein-ligand complex. The complex was solvated using the explicit TIP3P (Jorgensen et al., 1983) water model, which extended a minimum 10-Å distance from the box surface to any atom of the solute. Two consecutive steps of minimization were carried out. All bond lengths were constrained using the SHAKE algorithm (Ryckaert et al., 1977), and the equations of motion were integrated with a 2-fs time step using the Verlet leapfrog algorithm. To eliminate possible bumps between the solute and the solvent, the entire system was minimized in two steps. First, the complex was restrained with a harmonic potential with a force constant $k = 50$ kcal mol^{-1} Å^{-2}. The water molecules and counter ions were optimized using the steepest descent method of 1,000 steps, followed by the conjugate gradient method for 2,000 steps. Second, the entire system was optimized using the first step method without any constraints. Subsequently, the entire system was heated gradually in the NVT ensemble from 0 to 300 K over 400 ps, with a weak restraint ($k = 5$ kcal mol^{-1} Å^{-2}) for the complex (Wu et al., 2016). The final coordinates, obtained after the temperature equilibration simulation, were used for a 120-ns MD simulation, during which the temperature was kept by the Langevin thermostat with a collision frequency of 2 ps^{-1}. A constant pressure periodic boundary was used to maintain the pressure of the system using an isotropic position scaling algorithm with a relaxation time of 2 ps. After MD simulation, distances between two atoms were calculated using the cpptraj program, and the dictionary of secondary structure of protein program developed by Kabsch and Sander (1983) was used to assign the secondary structures of the BRI1-BAK1-BL complex. All the structure figures were prepared using PyMol (www.pymol.org).

Sequence Analysis

For sequence analysis, the sequences of 70 BRI1s or BRLs from 18 flowering plants and 223 LRR-RLK sequences from Arabidopsis were downloaded and analyzed in MEGA software (http://www.megasoftware.net/). The final alignment data were generated to a logo (Fig. 9; Supplemental Fig. S4) on the WebLogo Web site (http://weblogo.berkeley.edu/logo.cgi).

Supplemental Data

The following supplemental materials are available.

Supplemental Figure S1. Eighty-three total mutations of *BRI1* identified in this study and 22 previously reported *bri1* mutants.

Supplemental Figure S2. Overexpression of *mBAK1* in *bri1-5* resulted in a dominant negative phenotype.

Supplemental Figure S3. Monitoring of the equilibration of the MD trajectories of the wild-type complex and the BRI1-Pro-719Leu complex.

Supplemental Figure S4. Sequence analyses of the BRI1 activation loop.

Supplemental Figure S5. Endo H cleavage of BRI1 and responses of BES1 phosphorylation and *CPD* expression to BL treatment showed no significant differences between shoots and roots of *bri1-706* seedlings.

Supplemental Figure S6. Endo H analysis indicated that BRI1 is not retained in the ER in *bri1-710* and *bri1-711* and is partially retained in the ER in *bri1-705* and *bri1-706*.

Supplemental Figure S7. In *bri1-709*, the mutation results in a premature stop codon.

Supplemental Table S1. List of primers and enzymes used in this study for genotyping *bri1* TILLING mutations.

ACKNOWLEDGMENTS

We thank J.L. laboratory member Yao Xiao for generating the BES1 antibody and Steven Henikoff and his team for their hard work on the Arabidopsis TILLING project.

Received January 30, 2017; accepted April 27, 2017; published May 1, 2017.

LITERATURE CITED

Asami T, Min YK, Nagata N, Yamagishi K, Takatsuto S, Fujioka S, Murofushi N, Yamaguchi I, Yoshida S (2000) Characterization of brassinazole, a triazole-type brassinosteroid biosynthesis inhibitor. Plant Physiol **123:** 93–100

Belkhadir Y, Durbak A, Wierzba M, Schmitz RJ, Aguirre A, Michel R, Rowe S, Fujioka S, Tax FE (2010) Intragenic suppression of a trafficking-defective brassinosteroid receptor mutant in Arabidopsis. Genetics **185:** 1283–1296

Bell EM, Lin WC, Husbands AY, Yu L, Jaganatha V, Jablonska B, Mangeon A, Neff MM, Girke T, Springer PS (2012) Arabidopsis lateral organ boundaries negatively regulates brassinosteroid accumulation to limit growth in organ boundaries. Proc Natl Acad Sci USA **109:** 21146–21151

Case DA, Cheatham TE III, Darden T, Gohlke H, Luo R, Merz KM Jr, Onufriev A, Simmerling C, Wang B, Woods RJ (2005) The Amber biomolecular simulation programs. J Comput Chem **26:** 1668–1688

Chaiwanon J, Wang ZY (2015) Spatiotemporal brassinosteroid signaling and antagonism with auxin pattern stem cell dynamics in Arabidopsis roots. Curr Biol **25:** 1031–1042

Cheng Y, Zhu W, Chen Y, Ito S, Asami T, Wang X (2014) Brassinosteroids control root epidermal cell fate via direct regulation of a MYB-bHLH-WD40 complex by GSK3-like kinases. eLife **3:** e02525

Clough SJ, Bent AF (1998) Floral dip: a simplified method for Agrobacterium-mediated transformation of *Arabidopsis thaliana*. Plant J **16:** 735–743

Clouse SD (1996) Molecular genetic studies confirm the role of brassinosteroids in plant growth and development. Plant J **10:** 1–8

Clouse SD, Langford M, McMorris TC (1996) A brassinosteroid-insensitive mutant in *Arabidopsis thaliana* exhibits multiple defects in growth and development. Plant Physiol **111:** 671–678

Clouse SD, Sasse JM (1998) Brassinosteroids: essential regulators of plant growth and development. Annu Rev Plant Physiol Plant Mol Biol **49:** 427–451

Domagalska MA, Schomburg FM, Amasino RM, Vierstra RD, Nagy F, Davis SJ (2007) Attenuation of brassinosteroid signaling enhances FLC expression and delays flowering. Development **134:** 2841–2850

Friedrichsen DM, Joazeiro CA, Li J, Hunter T, Chory J (2000) Brassinosteroid-insensitive-1 is a ubiquitously expressed leucine-rich repeat receptor serine/threonine kinase. Plant Physiol **123:** 1247–1256

Gendron JM, Liu JS, Fan M, Bai MY, Wenkel S, Springer PS, Barton MK, Wang ZY (2012) Brassinosteroids regulate organ boundary formation in the shoot apical meristem of Arabidopsis. Proc Natl Acad Sci USA **109:** 21152–21157

González-García MP, Vilarrasa-Blasi J, Zhiponova M, Divol F, Mora-García S, Russinova E, Caño-Delgado AI (2011) Brassinosteroids control meristem size by promoting cell cycle progression in Arabidopsis roots. Development **138:** 849–859

Gou X, Yin H, He K, Du J, Yi J, Xu S, Lin H, Clouse SD, Li J (2012) Genetic evidence for an indispensable role of somatic embryogenesis receptor kinases in brassinosteroid signaling. PLoS Genet **8:** e1002452

Gudesblat GE, Russinova E (2011) Plants grow on brassinosteroids. Curr Opin Plant Biol **14:** 530–537

Gudesblat GE, Schneider-Pizoń J, Betti C, Mayerhofer J, Vanhoutte I, van Dongen W, Boeren S, Zhiponova M, de Vries S, Jonak C, et al (2012) SPEECHLESS integrates brassinosteroid and stomata signalling pathways. Nat Cell Biol **14:** 548–554

Guo Z, Fujioka S, Blancaflor EB, Miao S, Gou X, Li J (2010) TCP1 modulates brassinosteroid biosynthesis by regulating the expression of the key biosynthetic gene DWARF4 in *Arabidopsis thaliana*. Plant Cell **22:** 1161–1173

Hacham Y, Holland N, Butterfield C, Ubeda-Tomas S, Bennett MJ, Chory J, Savaldi-Goldstein S (2011) Brassinosteroid perception in the epidermis controls root meristem size. Development **138:** 839–848

Hong Z, Jin H, Tzfira T, Li J (2008) Multiple mechanism-mediated retention of a defective brassinosteroid receptor in the endoplasmic reticulum of Arabidopsis. Plant Cell **20:** 3418–3429

Hong Z, Kajiura H, Su W, Jin H, Kimura A, Fujiyama K, Li J (2012) Evolutionarily conserved glycan signal to degrade aberrant brassinosteroid receptors in Arabidopsis. Proc Natl Acad Sci USA **109:** 11437–11442

Hornak V, Abel R, Okur A, Strockbine B, Roitberg A, Simmerling C (2006) Comparison of multiple Amber force fields and development of improved protein backbone parameters. Proteins **65:** 712–725

Hothorn M, Belkhadir Y, Dreux M, Dabi T, Noel JP, Wilson IA, Chory J (2011) Structural basis of steroid hormone perception by the receptor kinase BRI1. Nature **474:** 467–471

Jin H, Hong Z, Su W, Li J (2009) A plant-specific calreticulin is a key retention factor for a defective brassinosteroid receptor in the endoplasmic reticulum. Proc Natl Acad Sci USA **106:** 13612–13617

Jin H, Yan Z, Nam KH, Li J (2007) Allele-specific suppression of a defective brassinosteroid receptor reveals a physiological role of UGGT in ER quality control. Mol Cell **26:** 821–830

Jorgensen WL, Chandrasekhar J, Madura JD, Impey R, Klein ML (1983) Comparison of simple potential functions for simulating liquid water. J Chem Phys **79:** 926–935

Kabsch W, Sander C (1983) Dictionary of protein secondary structure: pattern recognition of hydrogen-bonded and geometrical features. Biopolymers **22:** 2577–2637

Kim TW, Michniewicz M, Bergmann DC, Wang ZY (2012) Brassinosteroid regulates stomatal development by GSK3-mediated inhibition of a MAPK pathway. Nature **482:** 419–422

Kwon M, Choe S (2005) Brassinosteroid biosynthesis and dwarf mutants. J Plant Biol **48:** 1–15

Li J, Chory J (1997) A putative leucine-rich repeat receptor kinase involved in brassinosteroid signal transduction. Cell **90:** 929–938

Li J, Lease KA, Tax FE, Walker JC (2001a) BRS1, a serine carboxypeptidase, regulates BRI1 signaling in *Arabidopsis thaliana*. Proc Natl Acad Sci USA **98:** 5916–5921

Li J, Nam KH, Vafeados D, Chory J (2001b) BIN2, a new brassinosteroid-insensitive locus in Arabidopsis. Plant Physiol **127:** 14–22

Li J, Wen J, Lease KA, Doke JT, Tax FE, Walker JC (2002) BAK1, an Arabidopsis LRR receptor-like protein kinase, interacts with BRI1 and modulates brassinosteroid signaling. Cell **110:** 213–222

Liu Y, Zhang C, Wang D, Su W, Liu L, Wang M, Li J (2015) EBS7 is a plant-specific component of a highly conserved endoplasmic reticulum-associated degradation system in Arabidopsis. Proc Natl Acad Sci USA **112:** 12205–12210

McCallum CM, Comai L, Greene EA, Henikoff S (2000) Targeting induced local lesions in genomes (TILLING) for plant functional genomics. Plant Physiol **123:** 439–442

Mora-García S, Vert G, Yin Y, Caño-Delgado A, Cheong H, Chory J (2004) Nuclear protein phosphatases with Kelch-repeat domains modulate the response to brassinosteroids in Arabidopsis. Genes Dev **18:** 448–460

Nam KH, Li J (2002) BRI1/BAK1, a receptor kinase pair mediating brassinosteroid signaling. Cell **110:** 203–212

Neff MM, Neff JD, Chory J, Pepper AE (1998) dCAPS, a simple technique for the genetic analysis of single nucleotide polymorphisms: experimental applications in *Arabidopsis thaliana* genetics. Plant J **14:** 387–392

Neff MM, Turk E, Kalishman M (2002) Web-based primer design for single nucleotide polymorphism analysis. Trends Genet **18:** 613–615

Noguchi T, Fujioka S, Choe S, Takatsuto S, Yoshida S, Yuan H, Feldmann KA, Tax FE (1999) Brassinosteroid-insensitive dwarf mutants of Arabidopsis accumulate brassinosteroids. Plant Physiol **121:** 743–752

Oh MH, Ray WK, Huber SC, Asara JM, Gage DA, Clouse SD (2000) Recombinant brassinosteroid insensitive 1 receptor-like kinase autophosphorylates on serine and threonine residues and phosphorylates a conserved peptide motif in vitro. Plant Physiol **124:** 751–766

Ryckaert J, Ciccotti G, Berendsen HJC (1977) Numerical integration of the cartesian equations of motion of a system with constraints: molecular dynamics of n-alkanes. J Comput Phys **23:** 327–341

Santiago J, Henzler C, Hothorn M (2013) Molecular mechanism for plant steroid receptor activation by somatic embryogenesis co-receptor kinases. Science **341:** 889–892

Shang Y, Lee MM, Li J, Nam KH (2011) Characterization of cp3 reveals a new bri1 allele, bri1-120, and the importance of the LRR domain of BRI1 mediating BR signaling. BMC Plant Biol **11:** 8

She J, Han Z, Kim TW, Wang J, Cheng W, Chang J, Shi S, Wang J, Yang M, Wang ZY, et al (2011) Structural insight into brassinosteroid perception by BRI1. Nature **474:** 472–476

Steber CM, McCourt P (2001) A role for brassinosteroids in germination in Arabidopsis. Plant Physiol **125:** 763–769

Su W, Liu Y, Xia Y, Hong Z, Li J (2011) Conserved endoplasmic reticulum-associated degradation system to eliminate mutated receptor-like kinases in Arabidopsis. Proc Natl Acad Sci USA **108:** 870–875

Su W, Liu Y, Xia Y, Hong Z, Li J (2012) The Arabidopsis homolog of the mammalian OS-9 protein plays a key role in the endoplasmic reticulum-associated degradation of misfolded receptor-like kinases. Mol Plant **5:** 929–940

Sun Y, Fan XY, Cao DM, Tang W, He K, Zhu JY, He JX, Bai MY, Zhu S, Oh E, et al (2010) Integration of brassinosteroid signal transduction with the transcription network for plant growth regulation in Arabidopsis. Dev Cell **19:** 765–777

Sun Y, Han Z, Tang J, Hu Z, Chai C, Zhou B, Chai J (2013) Structure reveals that BAK1 as a co-receptor recognizes the BRI1-bound brassinolide. Cell Res **23:** 1326–1329

Taylor I, Seitz K, Bennewitz S, Walker JC (2013) A simple in vitro method to measure autophosphorylation of protein kinases. Plant Methods **9:** 22

Till BJ, Reynolds SH, Greene EA, Codomo CA, Enns LC, Johnson JE, Burtner C, Odden AR, Young K, Taylor NE, et al (2003) Large-scale discovery of induced point mutations with high-throughput TILLING. Genome Res **13:** 524–530

Vert G, Nemhauser JL, Geldner N, Hong F, Chory J (2005) Molecular mechanisms of steroid hormone signaling in plants. Annu Rev Cell Dev Biol **21:** 177–201

Vilarrasa-Blasi J, González-García MP, Frigola D, Fàbregas N, Alexiou KG, López-Bigas N, Rivas S, Jauneau A, Lohmann JU, Benfey PN, et al (2014) Regulation of plant stem cell quiescence by a brassinosteroid signaling module. Dev Cell **30:** 36–47

Wang J, Jiang J, Wang J, Chen L, Fan SL, Wu JW, Wang X, Wang ZX (2014) Structural insights into the negative regulation of BRI1 signaling by BRI1-interacting protein BKI1. Cell Res **24:** 1328–1341

Wang J, Wolf RM, Caldwell JW, Kollman PA, Case DA (2004) Development and testing of a general Amber force field. J Comput Chem **25:** 1157–1174

Wang X, Chory J (2006) Brassinosteroids regulate dissociation of BKI1, a negative regulator of BRI1 signaling, from the plasma membrane. Science **313:** 1118–1122

Wang X, Kota U, He K, Blackburn K, Li J, Goshe MB, Huber SC, Clouse SD (2008) Sequential transphosphorylation of the BRI1/BAK1 receptor kinase complex impacts early events in brassinosteroid signaling. Dev Cell **15:** 220–235

Wang X, Li X, Meisenhelder J, Hunter T, Yoshida S, Asami T, Chory J (2005) Autoregulation and homodimerization are involved in the activation of the plant steroid receptor BRI1. Dev Cell **8:** 855–865

Wang Y, Sun S, Zhu W, Jia K, Yang H, Wang X (2013) Strigolactone/MAX2-induced degradation of brassinosteroid transcriptional effector BES1 regulates shoot branching. Dev Cell **27:** 681–688

Wang ZY, Bai MY, Oh E, Zhu JY (2012) Brassinosteroid signaling network and regulation of photomorphogenesis. Annu Rev Genet **46:** 701–724

Wang ZY, Seto H, Fujioka S, Yoshida S, Chory J (2001) BRI1 is a critical component of a plasma-membrane receptor for plant steroids. Nature **410:** 380–383

Wei Z, Li J (2016) Brassinosteroids regulate root growth, development, and symbiosis. Mol Plant **9:** 86–100

Wu D, Tao X, Chen ZP, Han JT, Jia WJ, Zhu N, Li X, Wang Z, He YX (2016) The environmental endocrine disruptor p-nitrophenol interacts with FKBP51, a positive regulator of androgen receptor and inhibits androgen receptor signaling in human cells. J Hazard Mater **307:** 193–201

Xu W, Huang J, Li B, Li J, Wang Y (2008) Is kinase activity essential for biological functions of BRI1? Cell Res **18:** 472–478

Yin Y, Vafeados D, Tao Y, Yoshida S, Asami T, Chory J (2005) A new class of transcription factors mediates brassinosteroid-regulated gene expression in Arabidopsis. Cell **120:** 249–259

Yin Y, Wang ZY, Mora-Garcia S, Li J, Yoshida S, Asami T, Chory J (2002) BES1 accumulates in the nucleus in response to brassinosteroids to regulate gene expression and promote stem elongation. Cell **109:** 181–191

Yu X, Li L, Zola J, Aluru M, Ye H, Foudree A, Guo H, Anderson S, Aluru S, Liu P, et al (2011) A brassinosteroid transcriptional network revealed by genome-wide identification of BESI target genes in *Arabidopsis thaliana*. Plant J **65:** 634–646

Yuan T, Fujioka S, Takatsuto S, Matsumoto S, Gou X, He K, Russell SD, Li J (2007) BEN1, a gene encoding a dihydroflavonol 4-reductase (DFR)-like protein, regulates the levels of brassinosteroids in *Arabidopsis thaliana*. Plant J **51:** 220–233

Zhang C, Xu Y, Guo S, Zhu J, Huan Q, Liu H, Wang L, Luo G, Wang X, Chong K (2012) Dynamics of brassinosteroid response modulated by negative regulator LIC in rice. PLoS Genet **8:** e1002686

Zhao B, Lv M, Feng Z, Campbell T, Liscum E, Li J (2016) TWISTED DWARF 1 associates with BRASSINOSTEROID-INSENSITIVE 1 to regulate early events of the brassinosteroid signaling pathway. Mol Plant **9:** 582–592

Zhou A, Wang H, Walker JC, Li J (2004) BRL1, a leucine-rich repeat receptor-like protein kinase, is functionally redundant with BRI1 in regulating Arabidopsis brassinosteroid signaling. Plant J **40:** 399–409

Zhu JY, Sae-Seaw J, Wang ZY (2013) Brassinosteroid signalling. Development **140:** 1615–1620